

Effect of the Madden–Julian Oscillation and Quasi-Biennial Oscillation on the Dynamics of Extratropical Stratosphere

K. K. Kandieva^{a, *}, O. G. Aniskina^a, A. I. Pogoreltsev^{a, b}, O. S. Zorkaltseva^c, and V. I. Mordvinov^{c, d}

^a*Russian State Hydrometeorological University, St. Petersburg, Russia*

^b*St. Petersburg State University, St. Petersburg, Russia*

^c*Institute of Solar–Terrestrial Physics, Siberian Branch, Russian Academy of Sciences, Irkutsk, Russia*

^d*Irkutsk State University, Irkutsk, Russia*

**e-mail: kanykeikandieva@gmail.com*

Received March 17, 2018; revised March 17, 2018; accepted May 25, 2018

Abstract—The effects of the Madden–Julian oscillation and quasi-biennial oscillation in the equatorial stratosphere on the dynamic processes in the extratropical stratosphere has been studied with the use of a model of the middle and upper atmospheric circulation. The heat source of the Madden–Julian oscillation in tropics is specified as a longitude-modulated wave perturbation with a zonal wavenumber of $m = 2$ and a period of about $T = 45$ days that propagates eastward with a phase speed of ~ 5 m/s. Ensemble calculations were carried out independently for the westerly and easterly phases of the quasi-biennial oscillation. Analysis of the results has shown that both phenomena strongly affect the circulation of the winter extratropical stratosphere, the polar vortex decay, and sudden stratospheric warming events; the character of the effect depends on the combination of their phases. The good agreement between the simulation results and the reanalysis of data confirms our results.

DOI: 10.1134/S0016793218060063

1. INTRODUCTION

A large amount of data on the parameters of the middle atmosphere (10–100 km) has been gathered to date due to ground-based and satellite sounding information. The intra-annual variations of the middle atmosphere caused by seasonal variations in the insolation is well studied. However, the nature and process of the development of strong disturbances of the winter circulation, i.e., sudden stratospheric warming events (SSWs), remain understudied, even though nearly all SSW events occurring in the Southern and Northern Hemispheres since 1960s have been analyzed based on observational data and reanalysis archives (Palmeiro et al., 2015; Butler et al., 2017; Chiodo and Polvani, 2017; Ivy et al., 2017; Grise and Polvani, 2017). The dates of the main SSW events observed in 1958–2013 have been tabulated (e.g., Butler and Gerber, 2018).

According to the conventional view, stratospheric polar vortex decay and SSW events are caused by the propagation of stationary planetary waves (SPWs) into the stratosphere (Matsuno, 1971). This is confirmed by observation results and the simulation of SPW interaction with the mean flow in the stratosphere and mesosphere (Chandran et al., 2014; Liu and Roble, 2002; Smith, 1983; Plumb, 1985). A stable correlation between the polar vortex variability in the strato-

sphere, the SPW in the troposphere, and annual modes was discovered (Gerber and Polvani, 2009). The effect of SPWs with wavenumbers of $m = 1$ and 2 (SPW1 and SPW2) on the dynamics of the stratosphere was discussed (Sheshadri et al., 2015). However, inverse effects of the circulation variations during SSW events on the propagation of planetary waves and the correlation between different atmospheric layers (troposphere–stratosphere–mesosphere) remain unclear. This leads researchers to increase the vertical resolution of model calculations and to adopt a large amount of stratospheric data during the simulation of dynamic processes in the middle atmosphere (Gerber et al., 2012).

The simulation results show that anomalies in stratospheric circulation and SSWs can result from the oscillation and interference of normal atmospheric modes at stratospheric altitudes (Pogoreltsev, 2007). Analysis of SSW events based on observational data allowed the determination of the periodicity and succession in SSW development, which not only confirms this point of view but also complicates the general pattern of SSW development (Pogoreltsev et al., 2015). It turns out that the polar vortex decay in the stratosphere is preceded by a chain of events: the vortex activity in the stratosphere increases two to three weeks before the SSW, and the vortex penetrates the

stratosphere in Northern Atlantic; synoptic processes activate, and the vortex activity intensifies in the eastward direction. Wavetrains in synoptic representation over Northern Eurasia, which determine the vortex activity, often precede the formation of blockings and large-scale weather anomalies over Eurasia (Palmen and Newton, 1973). Intensification of the synoptic activity in the eastern part of Eurasia results in an increase in vortex flows in the stratosphere over Eastern Asia and Northern Pacific with time. Nonlinear interactions between SPWs and the polar vortex and stationary anticyclone in the stratosphere result in the polar vortex decay and a strong major warming.

The actual pattern of SSW development apparently includes a complex of processes: free mode in the middle atmosphere and external forces induced by different factors, which can be more or less interpreted in terms of planetary wave propagation and interaction with the mean flow. There is evidence that the circulation in the polar stratosphere is affected by orographic stationary waves (Gavrilov et al., 2018), quasi-biennial oscillation (QBO), tropospheric blockings, and traveling waves (Kochetkov et al., 2014).

Another possible source of effects on the circulation in the extratropic stratosphere is a convection anomaly in the tropic troposphere, which can be caused by El Niño–Southern Oscillation (ENSO) or Madden–Julian oscillation (MJO). It was ascertained (Taguchi and Hartmann, 2006) that the temperature decreases in the tropic stratosphere and increase in the polar stratosphere during the warm ENSO phase. The situation is reversed during La Niña. However, the estimation of the correlation between ENSO and SSWs by Butler and Polvani (2011) did not reveal this rule. SSW events were observed during different ENSO phases with equal probability. The authors explained the discrepancy between their results and those results from Taguchi and Hartmann (2006) by the fact that SSWs are rare extreme events and are lost against the background of the total dynamics of the stratosphere. The effect of the QBO phase on SSWs turns out to be more significant. Independently of the QBO phase, SSW events occur more often during the easterly QBO phase. The possibility of predicting the QBO phase (Gabis and Troshichev, 2011) can significantly increase the probability of forecasting SSWs and weather anomalies in the troposphere connected with SSWs.

The MJO phenomenon is less studied. It is a source of disturbances in the low latitudes troposphere and is the oscillation of weather fields with a period of 30–60 day (Madden and Julian, 1971, 1972). MJO is clearly shown in the dynamics of deep convection and the amount of precipitation; it is a longitude-localized wave that propagates eastward with an average phase speed of ~5 m/s (Weickmann et al., 1985) over the Indian and Pacific Oceans. The development of a large-scale convective MJO cell begins in the west of

the Indian Ocean; the deep convection zone then moves to the east, gradually damping as it moves towards the eastern Pacific. The convective cell again sometimes intensifies over the tropical Atlantic but with a smaller amplitude. The convective instability in the tropics is most often considered to be a cause of MJO, but it is proposed that the planetary waves that arrive at the tropics from the midlatitudes are initiated by MJO in a number of works (Ray and Zhang, 2010).

Torsional oscillations are indirect evidence of the MJO effect on stratospheric circulation, i.e., variations in the average zonal velocity component in a range of 10–20 days (Mordvinov et al., 2009, 2011, 2013). The matching of torsional oscillations and SSWs has shown that the latter is usually preceded by a period of increased activity of these oscillations in the tropical stratosphere; these oscillations propagate from the tropics to the midlatitudes for ~10 days. An increase in the temperature in the polar stratosphere almost exactly coincides with the time of arrival of disturbances in the region of stratospheric jet stream (Kochetkova et al., 2014).

The possibility of an MJO effect on the state of stratospheric polar vortex is confirmed by experiments with the general circulation model of the atmosphere (Garfinkel et al., 2014). According to the calculations, when the deep convection zone is passing over the western part of the equatorial Pacific, vortex heat fluxes from the convection zone to the troposphere and stratosphere over the northern Pacific intensify. This decreases the surface pressure in the troposphere and results in the polar vortex decay in the stratosphere. Note that the reproduction of SSWs in general circulation models are not completely satisfactory; in particular, the number of SSWs in the model of Institute of Computational Mathematics, Russian Academy of Sciences, is lower than that observed in reality (Vargin and Volodin, 2016). Accounting for MJO in forecast models allows the quality of the SSW forecast to be increased, with a lead-time of up to 20 days (Garfinkel and Schwartz, 2017). The effect of MJO phases on the polar vortex intensity was considered (Kandieva et al., 2018) based on the analysis of the MERRA archive data (Rienecker et al., 2011). It was shown that the MJO effect on the change in the stratospheric circulation depends on the geographic coordinates of the anomalies associated with this tropical oscillation; the polar stratospheric vortex increases during the strong MJO state of (in ~65% of cases), and its center shifts in the easterly direction.

The goal of this work is to use a model of the circulation of the middle and upper atmosphere (MUAM) to estimate the combined effect of two phenomena on the winter extratropical circulation in the stratosphere, the MJO in the equatorial troposphere, and the QBO of zonal wind in the equatorial stratosphere. The advantage of numerical experiments is the ability to exclude other factors that affect the dynamics of pro-

cesses in the extratropical stratosphere, e.g., interannual variations in meteorological fields in the midlatitude troposphere, which strongly affect winter processes in the stratosphere and/or the effect of the ENSO event on the middle atmosphere.

2. DESCRIPTION OF MODEL EXPERIMENTS

2.1. MUAM Model

The middle and upper atmosphere model (MUAM) has been used to simulate the thermal regime and general circulation of the atmosphere (Pogoreltsev et al., 2007). The MUAM model is a 3D nonlinear general circulation model of the atmosphere implemented on a mesh of 5.625° in longitude and 5° in latitude. The log-isobaric altitude $z = -H \ln(p/1000)$ (p is the pressure, hPa; $H = 7$ km) was used as a vertical coordinate. The altitude step $\Delta z = 0.4H$; it is possible to specify an arbitrary number of vertical levels from 48 to 60. In this work we used a 56-level version of the MUAM model; therefore, the upper boundary corresponds to a geopotential altitude of ~ 300 km. The time integration step was 225 s. The latest MUAM version includes new parameterizations: the effects of orographic gravity waves (Gavrilov and Koval, 2013) and normal atmospheric modes (Pogoreltsev et al., 2014). In addition, new climate distributions of ozone (Suvorova et al., 2017) and water vapor in the troposphere (Ermakova et al., 2017) that take into account longitudinal variations were used. The latitudinal–longitudinal distributions of the geopotential altitude of the 1000-hPa level and of the temperatures at this level, which were derived from the monthly average (January) data from the Japanese 55-year Reanalysis (JRA55), were used as lower boundary conditions (Kobayashi et al., 2015). To exclude the ENSO effect in the calculation of the lower boundary conditions, the distributions for 1982, 1991, 1994, 2002, and 2004, with neutral ENSO phase, in terms of the MEI index (Multivariate ENSO Index) (<http://www.esrl.noaa.gov/psd/enso/mei/table.html>), were averaged. The scheme of numerical experiments exactly corresponds to the scheme described in Pogoreltsev et al. (2007): a fixed zenith angle of Sun corresponding to the conditions of January 1 was used up to the 330th model day, and its seasonal variations were then included. Thus, the 330–400th model days corresponded to January–February and early March. Ensembles of ten solutions found with different initial conditions were obtained for all considered calculation variants.

2.2. QBO and MJO Implementation in the Model

During the simulation, the task was to determine the dependence of winter circulation anomalies in the extratropical stratosphere on the heat source in tropics; this simulated MJO during different QBO phases. The QBO effect was taken into account via the introduction of an additional term in the prognostic equa-

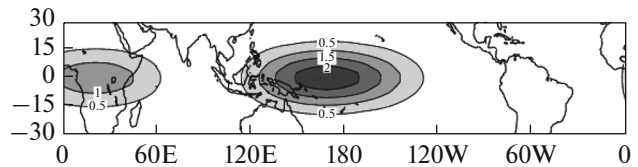


Fig. 1. Heated regions of MJO model corresponding to January 1.

tion for the zonal wind speed component proportional to the difference between the calculated and climatic distributions of the zonal average zonal wind speed for the westerly and easterly phases of QBO. The QBO phase for each year was determined by the sign of the deviation of the averaged zonal flow in January–February from the climatic one at an altitude of 30 km (10 hPa) (Pogoreltsev et al., 2014). The additional term was “included” in the latitude range 17.5° S– 17.5° N at altitudes of 0–50 km. An additional tropical heat source simulating the MJO effect was represented as a wave perturbation with a zonal wavenumber of $m = 2$ and a period of $T = 45$ days moving eastward with an average phase speed of ~ 5 m/s (see Introduction).

The following equation approximates the moving heat source:

$$Q(\lambda, \varphi, z, t) = A[1 + \cos(m\lambda - \omega t)] \times \exp\left(-\left(\frac{\lambda - \lambda_0}{\lambda_0}\right)^2 - \left(\frac{\varphi}{\varphi_0}\right)^2 - \left(\frac{z - z_0}{\Delta z}\right)^2\right),$$

where $A = 1.5$ K/day is the heating amplitude; the maximal heating falls to the longitude $\lambda_0 = 120^\circ$ E. The heating anomalies move along the equator and are limited by low latitudes $\varphi_0 = 15^\circ$. In the vertical profile, the heating maximum is at an altitude of $z_0 = 7$ km. The heating regions have an elliptical shape; their location in Fig. 1 corresponds to January 1 in the numerical experiments.

A similar shape of the MJO source, but in the form of geopotential disturbance at the bottom boundary, was used by Bao and Hartmann (2014), and it approximately corresponds to the observed MJO structure (Wheeler and Hendon, 2004; Kandjeva et al., 2017).

3. SIMULATION RESULTS

1. Figure 2 shows the differences between the average values of the zonal component of wind speed and air temperature during the westerly and easterly phases of QBO (isolines) without (a and b) and with inclusion (c and d) of MJO model. The distributions of the mean zonal characteristics are averaged over January–February. The gray color shows the distribution of the statistical significant distribution according to the Student’s t -test in the Welch modification (1947):

$$t = |\bar{X}_{\text{MJO}} - \bar{X}| / \left(S_{\text{MJO}}^2 / N_{\text{MJO}} + S^2 / N \right)^{1/2},$$

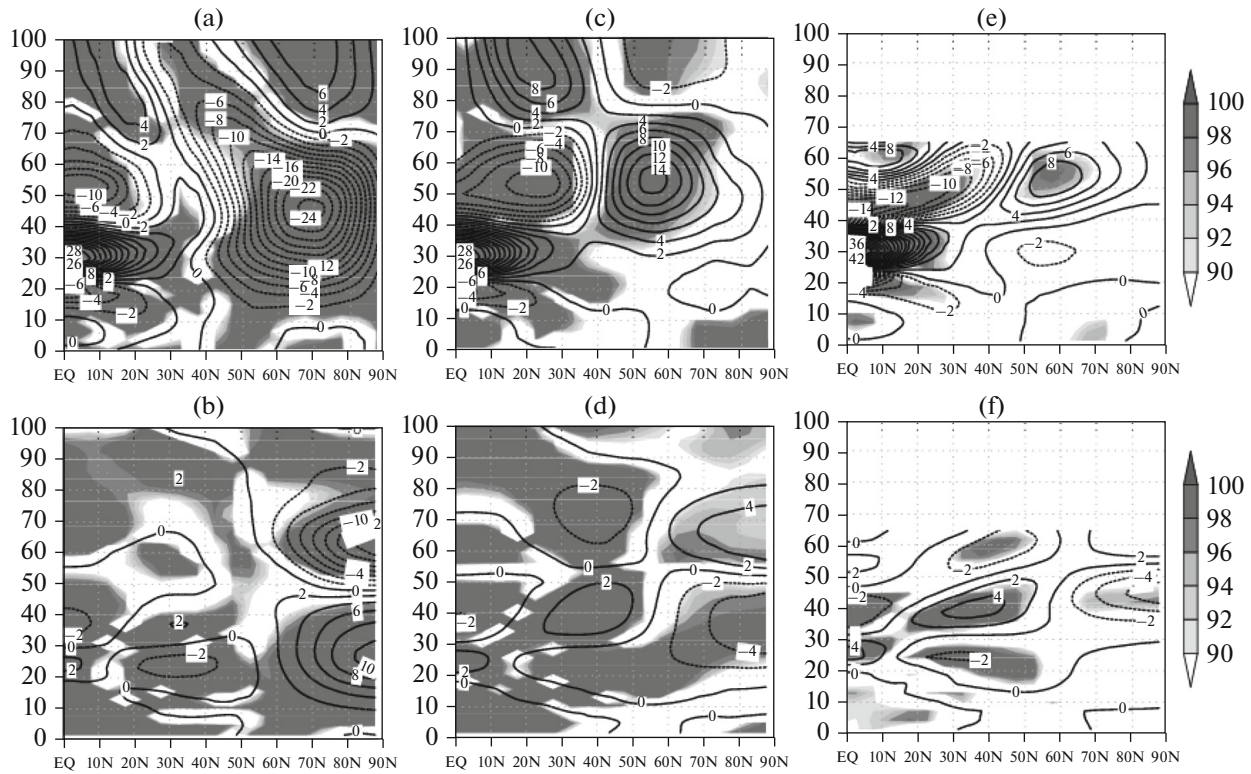


Fig. 2. Differences in the (a, c, e) zonal average wind velocity and (b, d, and f) zonal average air temperature during the westerly and easterly QBO phases: (a and b) model without MJO, (c and d) model with MJO, (e and f) calculations from MERRA reanalysis data. Gray regions show the statistically significant distributions (significance levels are designated in percents) of the differences according to the Student's *t*-test.

where \bar{X}_{MJO} and \bar{X} are the average values of meteorological parameters calculated for a fixed QBO phase with and without accounting for the additional MJO heat source; S_{MJO} and S are the standard deviations of the parameters; and N_{MJO} and N are the sample sizes. The number of degrees of freedom is calculated by the equation

$$v = \left(\frac{S_{\text{MJO}}^2}{N_{\text{MJO}}} + \frac{S^2}{N} \right)^2 \left/ \left[\frac{(S_{\text{MJO}}^2/N_{\text{MJO}})^2}{N_{\text{MJO}} - 1} + \frac{(S^2/N)^2}{N - 1} \right] \right.$$

Figures 2e and 2f give the difference between the values of the zonal average speed and air temperature during the westerly and easterly phases of QBO according to the MERRA archive data (Rienecker et al., 2011) for comparison. Positive deviations correspond to the westerly QBO phase, and negative values correspond to the easterly phase. As a result, the years with the westerly (1993, 1995, 1997, 1999, 2002, 2004, 2006, 2008, and 2011) and easterly (1994, 1998, 2000, 2001, 2003, 2005, 2007, 2010, and 2012) phases of QBO have been selected.

Analysis of the distributions constructed from the model data make it possible to estimate the effects of the factors (QBO and MJO) separately. In the absence

of an additional heat source at the equator, the effect of QBO phase on the polar stratospheric circulation turned out to be very strong (Fig. 2a): the velocities of the stratospheric jet stream at altitudes of 30–60 km during the westerly phase of QBO were 20–25 m/s lower than during the easterly phase of QBO. The differences in the zonal average temperatures (Fig. 2b) were also quite high and amounted to approximately +10 K at altitudes of 20–30 km and –10 K at altitudes of 60–70 km. The inclusion of MJO completely changes the character of the distributions: the differences in the zonal average velocity in the extratropical latitudes changes sign, become smaller in magnitude, and shifts southward by 10°–15° (Fig. 2c); the temperature anomalies weaken and change the sign in the polar region (Fig. 2d); the agreement with the MERRA archive data, which is shown in Figs. 2e and 2f, improves.

The next step is to compare the integral characteristics of MJO effect on the circulation of the extratropical stratosphere retrieved from model data and JRA55 reanalysis data.

To do this, we first summarize the distributions of the zonal average velocities and the zonal average temperature during the westerly and easterly QBO phases (20 realizations) obtained in experiments with MJO.

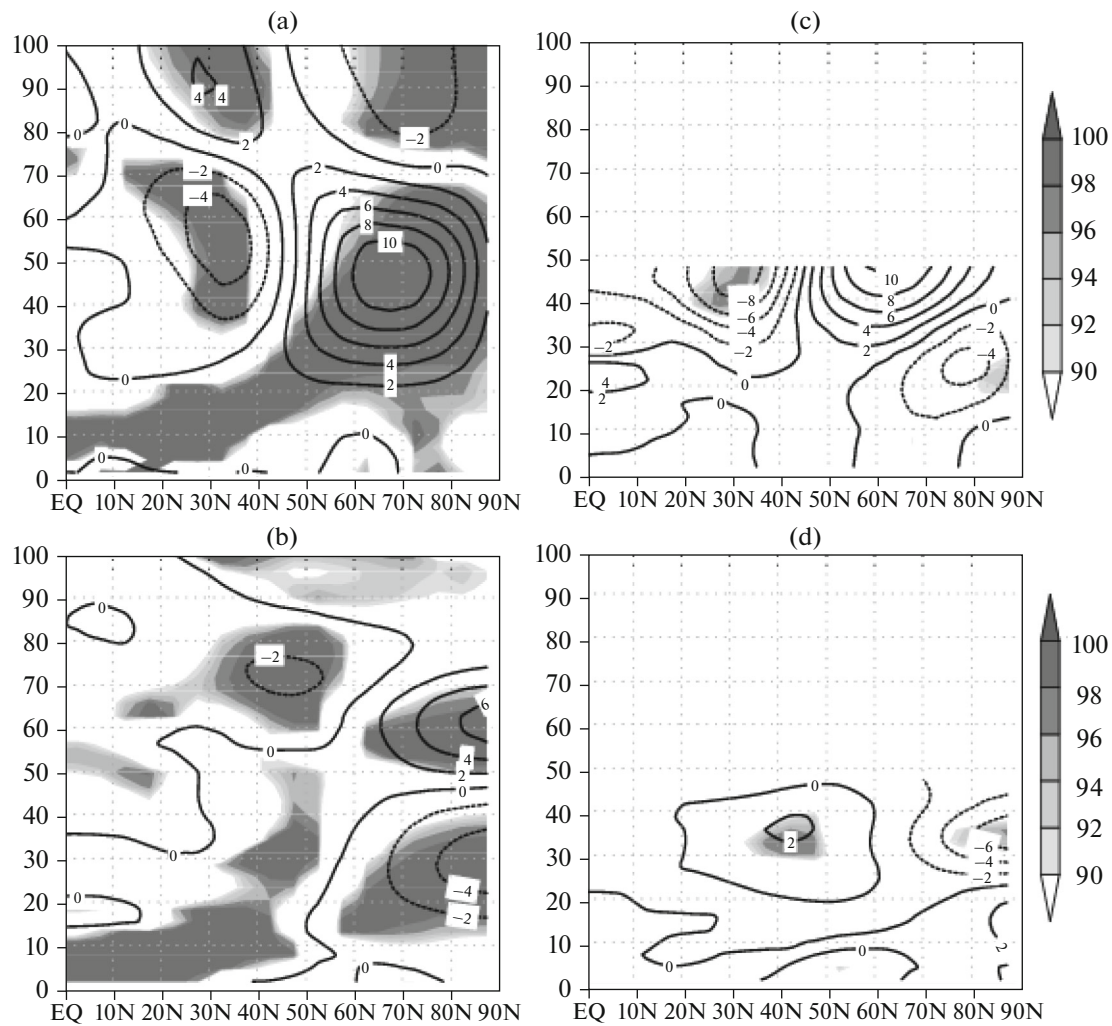


Fig. 3. Variations in the (a and c) zonal wind velocity and (b and d) air temperature induced by the MJO calculated with (a and b) model and (c and d) JRA55 data. Gray regions show statistically significant distributions (significance levels are designated in percents) of the differences according to the Student's *t*-test.

The resulting sums are then subtracted from the distributions obtained in experiments without MJO. Figures 3a and 3b show the calculation results. For comparison, Figs. 3c and 3d show the variations in these two parameters under the MJO effect derived from JRA data. The MJO effect is calculated as the difference between the meteorological fields in periods of high and low MJO intensity, regardless of the QBO phase. To estimate the intensity of the phenomenon, the MJO index for 1958–2016 was calculated from JRA reanalysis data with the method described by Wheeler and Hendon (2004). The MJO index used is characterized by two parameters: phase and amplitude. The MJO phase fixes the spatial position of cloudiness of MJO, and the amplitude is an indicator of the phenomenon intensity. Thus, the MJO effect is considered strong (weak) if the average amplitude over January–February in a particular year is higher (lower) than the average amplitude over the

entire studied period (59 years). As a result, years with strong (1959, 1970, 1979, 1985, 1988, 1989, 1994, 1997, 2004, and 2013) and weak MJO effect (1966, 1968, 1971, 1974, 1980, 1996, 1998, 1999, 2002, and 2003) have been selected, and the difference between their average values has been calculated.

The use of the integral characteristics for the comparison allows more accurate estimation of the actual climatic effect of MJO on the circulation in the extratropical stratosphere without division into the westerly and easterly phases of QBO.

The figures show the general correspondence between the distributions of the differences between the zonal average velocity and temperature obtained in numerical experiments and the distributions of the integral characteristics from the reanalysis archive data. The anomalies are also quite close. Unfortunately, the altitudes available for analysis from observational data are much lower than the altitude range in

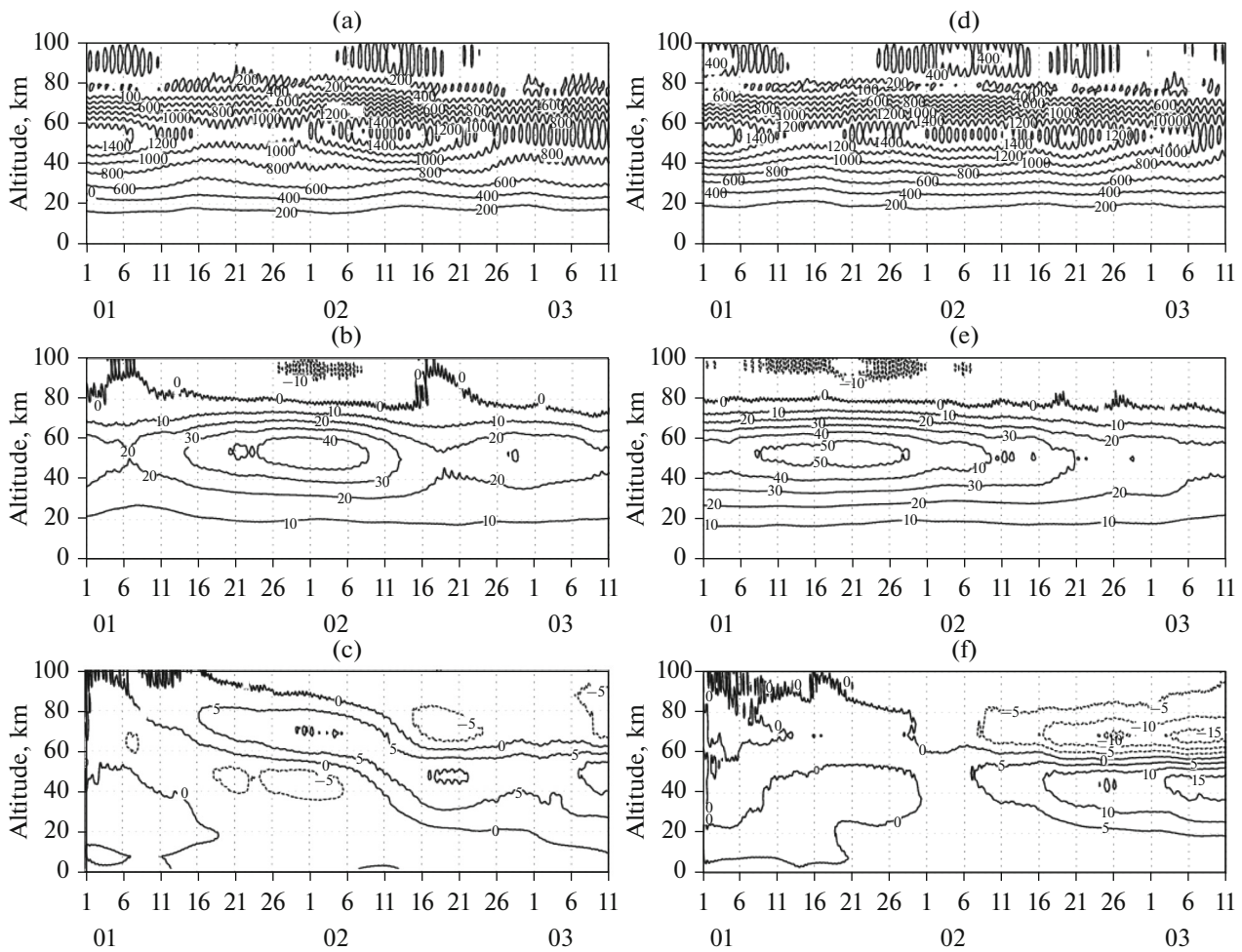


Fig. 4. Altitude-temporal sections calculated (a–c) without and (d–f) with accounting for the MJO: (a and d) SPW1 amplitudes in the geopotential altitude field at the latitude 62.5° N; (b and e) zonal average zonal stream velocity at the latitude 62.5° N; (c and f) zonal average air temperature at the latitude 87.5° N.

the MUAM model; hence, comparison above 50 km is impossible. At the altitudes available for comparison, the amplitudes of the integral anomalies of the zonal velocity and temperature turned out to be smaller than the anomalies of amplitudes during the westerly and easterly phases of QBO, i.e., the MJO effects on the circulation of the extratropical stratosphere are opposite during the easterly and westerly phases of QBO and leveled on average when the phases alternate.

A detailed analysis of variations in meteorological parameters in the polar stratosphere was performed with the use of altitude-temporal sections of the average values of the first zonal harmonic amplitude in the geopotential altitude field (SPW1), the zonal wind component at a latitude of 62.5° N, and the temperature in the polar stratosphere at 87.5° N for two calculation realizations: without (Figs. 4a–4c) and with accounting for MJO (Figs. 4d–4f). Analysis of the results showed that the SSW begins developing in early February at altitudes of 60–80 km, simultaneously with the enhancement of the zonal stream centered at

an altitude of ~ 55 km in the case without MJO; the temperature decreases at altitudes of 40–60 km. The temperature anomalies above and below the jet stream are 5–10 K in modulus. In the mid-February, the SPW1 amplitude increases, the zonal stream weakens, the heat penetrates to altitudes of 40–60 km, and the temperature decreases by 5 K relative to the background values at altitudes of 60–80 km.

The nature of the dynamic processes differs in the case with MJO. The stratospheric jet stream is stronger and stabler, and thermal anomalies are almost absent above and below the jet stream most of the time. In the second half of February, as in the experiment without MJO, the SPW1 amplitude increases and the jet stream weakens. Simultaneously, the thermal anomalies of different signs begin rising above and below an altitude of ~ 55 km; the anomaly maxima can attain 15 K. In general, the character of variations in the zonal average characteristics of the polar stratospheric circulation without MJO is oscillating: quasi-periodic intensification and weakening of the jet

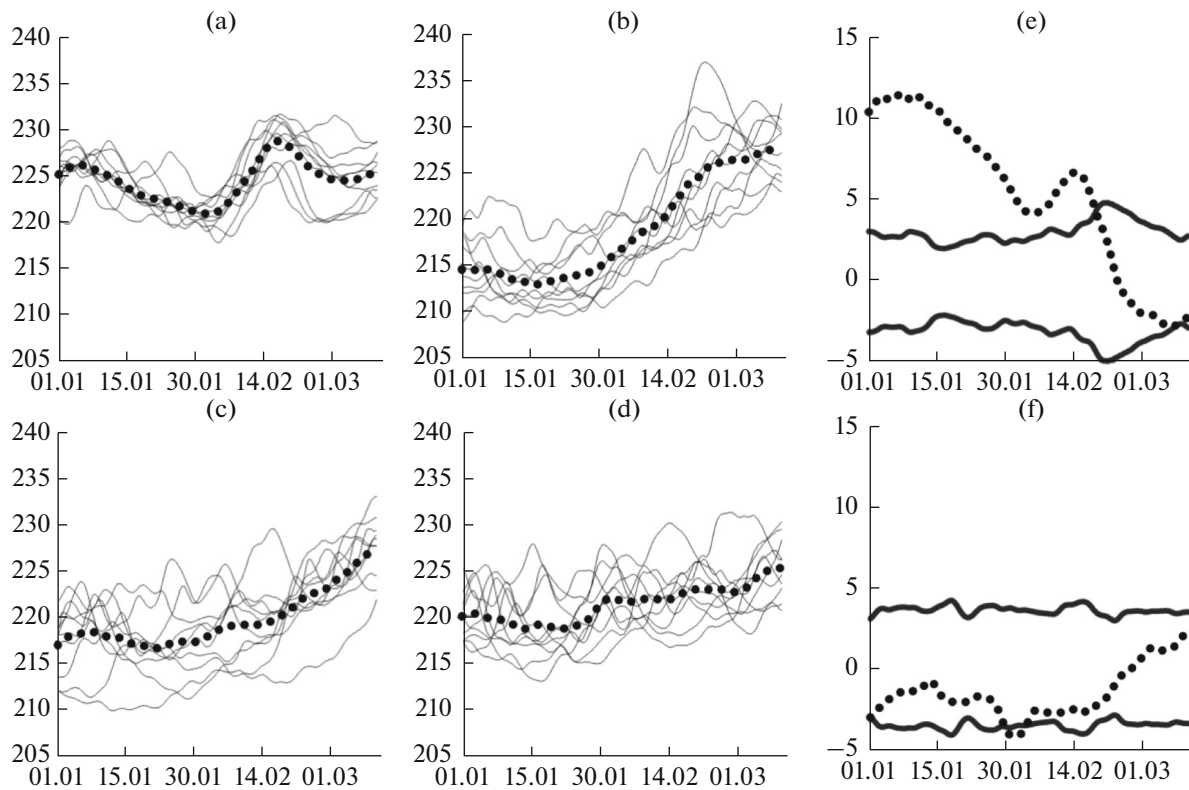


Fig. 5. Variations in the air temperature in the polar stratosphere during the (a and b) westerly and (c and d) easterly phases QBO (a and c) without and (b and d) with the inclusion of MJO at an altitude of 30 km; dots show the variations in the temperature averaged over ten model realizations. Curves of the differences in the ensemble average temperature values caused by the inclusion of MJO during the (e) westerly and (f) easterly QBO phases; solid curves on the right fragments limit the range of differences which correspond to the 95% significance level according to the Student's *t*-test.

stream are accompanied by sign-alternating temperature anomalies above and below it. The inclusion of MJO enhances and stabilizes the jet stream: the temperature anomalies above and below it weaken. SSWs tend to develop in late winter, have a higher temperature, and are not accompanied by vertical transfers.

2. Differences in the zonal averages of zonal velocity and temperature can be caused by variations in the parameters of the stratospheric polar vortex or by differences in SSW characteristics, or, more likely, by a combination of these factors. To verify these assumptions, we compared the time variations in the zonal average temperature at an altitude of 30 km in the latitude range 60° – 90° N in experiments with different QBO phases, with and without MJO. The average temperatures in these altitude and latitude ranges reflect quite well the dynamics of stratospheric processes during SSW.

Figures 5a–5d show the time variations in the zonal average air temperature in the high latitudes of the stratosphere during the westerly (a and b) and easterly (c and d) QBO phases without (a and c) and with accounting (b and d) for MJO heat source. Figures 5e and 5f show time variations in the temperature difference with and without MJO averaged over

ten realizations, as well as the curves of the temperature differences significant at a level of 95%. The time variations in the air temperature evidently change significantly with the QBO phase. During the westerly phase, the temperature increases due to the SSW, mainly in the first half of January and in the second half of February. During the easterly phase, the SSW is less regular and most often occurs at the end of the period. On average, the temperature of the polar stratosphere during the easterly QBO phase is lower than during the westerly phase. Inclusion of the MJO in the westerly QBO phase leads to a decrease in the number of SSWs: instead of two SSWs, only one event develops for the period from January 1 to March 15, and its onset is shifted to a later date in the second half of February. The MJO hardly affects the temperature regime of the polar stratosphere during the easterly QBO phase.

The average temperatures in the latitude range 60° – 90° N were also calculated at an altitude of 60 km. Figure 6 shows the results. Comparative analysis of the variations in the air temperature at the two altitudes during the westerly QBO phase without MJO showed that when maximal temperatures are observed at an altitude of 60 km (Fig. 6a) at the late January and mid-March; the temperatures at an altitude of 30 km are

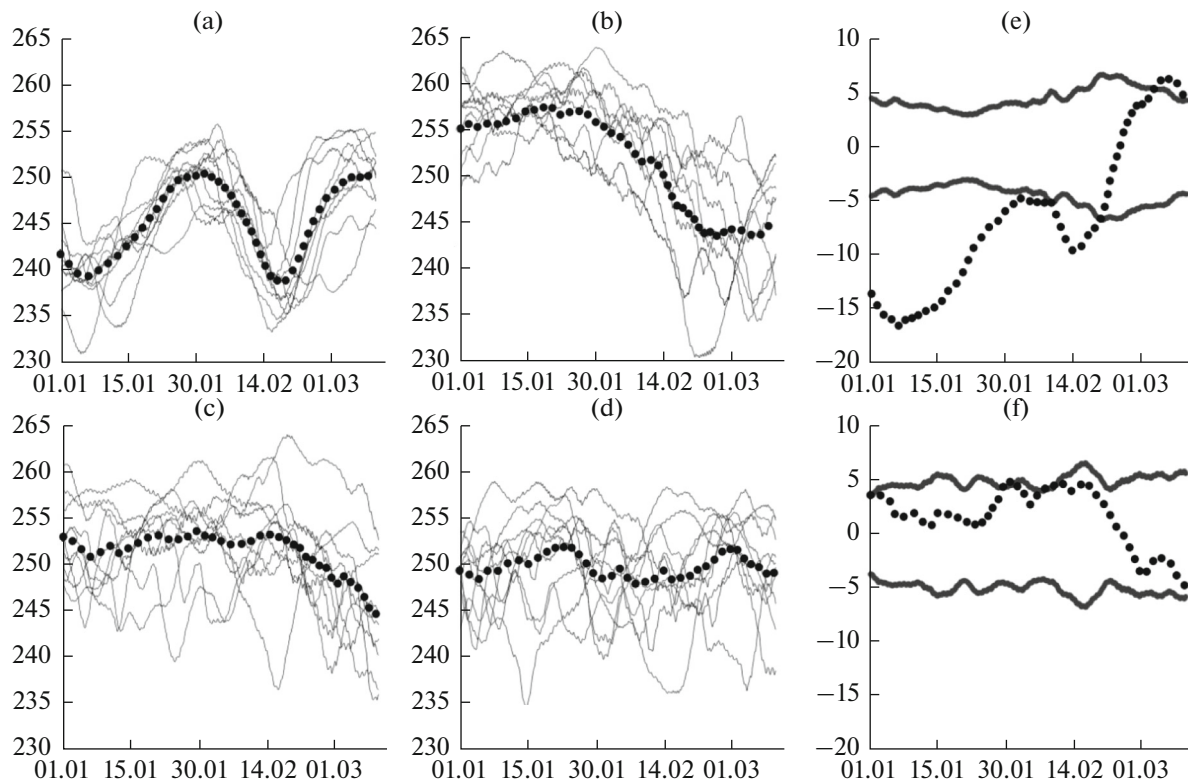


Fig. 6. The same as in Fig. 5 at an altitude of 60 km.

minimal (Fig. 5a). Conversely, the minimal temperatures at 60 km coincide with the SSW at 30 km. If the MJO is included in the calculations of temperature variations, only one temperature maximum is observed at 60 km (Fig. 6b), as is the case at 30 km (Fig. 5b), but it falls on the first half of the studied period. Comparative analysis of the temperature curves during the easterly QBO phase without (Fig. 6c) and with MJO (Fig. 6d) showed no variations in the temperature, neither in magnitude nor in behavior.

The qualitative conclusions are supported by statistical estimates. During the westerly QBO phase, the MJO significantly affects the temperature of the polar stratosphere during the most of the studied time interval. During the easterly QBO phase, this effect is small. The curves of the zonal average velocity (not shown) agree with the temperature variations. During the easterly QBO phase, the zonal average velocities in the polar stratosphere are on average higher than those during the westerly phase. The inclusion of MJO at the westerly QBO phase increases the zonal average velocity.

4. CONCLUSIONS

A series of experiments with and without an additional heat source that simulates the MJO effect on circulation in the troposphere and stratosphere were carried out separately for the westerly and easterly phases of QBO. They made it possible to analyze in

detail the MJO effect on the dynamics of processes in the extratropical stratosphere and the combined effect of two factors, MJO and QBO, during different phases.

Analysis of the results with and without taking into account the MJO effect on the of dynamic processes in the stratosphere shows that the polar vortex becomes stabler and the development of SSW shifts to a later date in the case of consideration of MJO. The SPW1 amplitude increases and the jet stream weakens during the SSW development. The region with positive zonal average temperature anomalies is located in the layer from 20 to ~55 km, and negative temperature anomalies are observed above this layer. At the maximum, the anomalies exceed the anomalies in the case without MJO and attain 15 K. Without MJO, variations in the zonal average parameters of circulation of the polar stratosphere are of an oscillatory nature: quasi-periodic intensification and weakening of the jet stream are accompanied by alternating temperature anomalies above and below it. Analysis shows that inclusion of the MJO enhances and stabilizes the polar vortex: the temperature anomalies above and below the jet stream weaken, and the SSWs tend to reach higher temperatures.

Analysis of the combined MJO and QBO effect shows that the temperature variations in the polar stratosphere are better expressed and have a larger

amplitude during the westerly QBO phase. SSWs caused by the polar vortex decay most often occur in the early and late winter. Analysis of the temperature variations in the lower mesosphere (60 km) revealed that SSW periods coincide with the periods of minimal temperatures in the lower mesosphere, and, conversely, temperature maxima are observed in the lower mesosphere in periods without SSWs. During the easterly QBO phase, SSWs can arbitrary occur in winter, both in the stratosphere and in the mesosphere.

It is still unclear how the MJO affects the circulation of the polar stratosphere. The MJO, which is a longitude-localized wave packet propagating eastward, can transfer a pulse to the mean zonal flow in the stratosphere, thus increasing its velocity and reducing the probability of SSW development. On the other hand, the MJO initiates convective heat transfer in the troposphere and stratosphere. Depending on the MJO phase, these transfers can either enhance or weaken the climatic ridge and anticyclone over the northern Pacific, which plays an important role in SSW development.

ACKNOWLEDGMENTS

The adjustment of the MUAM model, the ensemble calculations of the middle atmosphere circulation, and the analysis of the MERRA and JRA55 data were carried out with the financial support of the Russian Foundation for Basic Research (project no. 18-05-01050); processing and interpretation of the results was carried out within Program of Fundamental Scientific Research of State Academies for 2013–2020 no. II.16.1.2 FNI.

REFERENCES

- Bao, M. and Hartmann, D.L., The response to MJO-like forcing in a linear shallow-water model, *Geophys. Res. Lett.*, 2014, vol. 41, pp. 1322–1328. doi 10.1002/2013GL057683
- Butler, A.H. and Gerber, E.P., Optimizing the definition of a sudden stratospheric warming, *J. Clim.*, 2011, vol. 31, no. 6, pp. 2337–2344. doi 10.1175/CLI-D-17-0648.1
- Butler, A.H. and Polvani, L.M., El Niño, La Niña, and stratospheric sudden warmings: A reevaluation in light of the observational record, *Geophys. Res. Lett.*, 2011, vol. 38, L13807. doi 10.1029/2011GL048084
- Butler, A.H., Sjöberg, J.P., Seidel, D.J., and Rosenlof, K.H., A sudden stratospheric warming compendium, *Earth Syst. Sci. Data*, 2017, vol. 9, pp. 63–76. doi 10.5194/essd-9-63-2017
- Chandran, A., Collins, R.L., and Harvey, V.L., Stratosphere–mesosphere coupling during stratospheric sudden warming events, *Adv. Space Res.*, 2014, vol. 53, pp. 1265–1289.
- Chiodo, G. and Polvani, L.M., Reduced southern hemispheric circulation response to quadrupled CO₂ due to stratospheric ozone feedback, *Geophys. Res. Lett.*, 2017, vol. 44, no. 1, pp. 465–474.
- Ermakova, T.S., Statnaya, I.A., Fedulina, I.N., Suvorova, E.V., and Pogoreltsev, A.I., Three-dimensional semi-empirical climate model of water vapor distribution and its implementation to the radiation module of the middle and upper atmosphere model, *Russ. Meteorol. Hydrol.*, vol. 42, no. 9, pp. 594–600.
- Gabis, I.P. and Troshichev, O.A., The quasi-biennial oscillation in the equatorial stratosphere: Seasonal regularity in zonal wind changes, discrete QBO-cycle period and prediction of QBO-cycle duration, *Geomagn. Aeron. (Engl. Transl.)*, vol. 51, no. 4, pp. 501–512.
- Garfinkel, C.I., Benedict, J.J., and Maloney, E.D., Impact of the MJO on the boreal winter extratropical circulation, *Geophys. Res. Lett.*, 2014, vol. 41. doi 10.1002/2014GL061094
- Garfinkel, C.I. and Schwartz, C., MJO-related tropical convection anomalies lead to more accurate stratospheric vortex variability in subseasonal forecast models, *Geophys. Res. Lett.*, 2017, vol. 44, pp. 10054–10062. doi 10.1002/2017GL074470
- Gavrilov, N.M. and Koval, A.V., Parameterization of mesoscale stationary orographic wave forcing for use in numerical models of atmospheric dynamics, *Izv., Atmos. Ocean. Phys.*, 2013, vol. 49, no. 3, pp. 244–251.
- Gavrilov, N.M., Koval, A.V., Pogoreltsev, A.I., and Savenkova, E.N., Simulating planetary wave propagation to the upper atmosphere during stratospheric warming events at different mountain wave scenarios, *Adv. Space Res.*, 2018, vol. 61, no. 7, pp. 1819–1836. doi 10.1016/j.asr.2017.08.022
- Gerber, E.P. and Polvani, L.M., Stratosphere–troposphere coupling in a relatively simple AGCM: The importance of stratospheric variability, *J. Clim.*, 2009, vol. 22, pp. 1920–1933. doi 10.1175/2008JCLI2548.1
- Gerber, E.P., Butler, A., Calvo, N., et al., Assessing and understanding the impact of stratospheric dynamics and variability on the earth system, *Bull. Am. Meteorol. Soc.*, 2012, vol. 93, pp. 845–859. doi 10.1175/BAMS-D-11-00145
- Grise, K.M. and Polvani, L.M., Understanding the time scales of the tropospheric circulation response to abrupt CO₂ forcing in the Southern Hemisphere: Seasonality and the role of the stratosphere, *J. Clim.*, 2017, vol. 30, no. 21, pp. 8497–8515.
- Ivy, D.J., Hilgenbrink, C., Kinnison, D., et al., Observed changes in the Southern Hemispheric circulation in May, *J. Clim.*, 2017, vol. 30, no. 2, pp. 527–536.
- Kandieva, K.K., Pogoreltsev, A.I., and Aniskina, O.G., Model source of the Madden–Julian Oscillation generation, *RSHU Proceedings Journal*, 2017, no. 47, pp. 91–105.
- Kandieva, K.K., Anikina, O.G., and Pogoreltsev, A.I., Effect of the Madden–Julian Oscillation generation on the intensity and structure of the polar vortex, *RSHU Proceedings Journal*, 2018, no. 50, pp. 18–27.
- Kobayashi, S., Harada, Y., Ota, Y., et al., The JRA-55 reanalysis: General specifications and basic characteristics, *J. Meteorol. Soc. Jpn.*, 2015, vol. 93, no. 1, pp. 5–48. doi 10.2151/jmsj.2015-001
- Kochetkova, O.S., Mordvinov, V.I., and Rudneva, M.A., Analysis of the factors affecting the occurrence of

- stratospheric warming, *Opt. Atmos. Okeana*, 2014, vol. 27, no. 8, pp. 719–727.
- Liu, H.-L. and Roble, R.G., A study of a self-generated stratospheric sudden warming and its mesospheric–lower thermospheric impacts using the coupled TIME-GCM/CCM3, *J. Geophys. Res.*, 2002, vol. 107, no. D23, 4695. doi 10.1029/2001JD001533
- Madden, R.A. and Julian, P.R., Detection of a 40–50 day oscillation in the zonal wind in the tropical Pacific, *J. Atmos. Sci.*, 1971, vol. 28, pp. 702–708.
- Madden, R.A. and Julian, P.R., Description of global-scale circulation cells in the tropics with a 40–50 day period, *J. Atmos. Sci.*, 1972, vol. 29, pp. 1109–1123.
- Matsuno, T., A dynamical model of the stratosphere sudden warming, *J. Atmos. Sci.*, 1971, vol. 28, pp. 1479–1494. doi 10.1175/1520-0469(1971)028<1479:ADMOTS>2.0.CO;2
- Mordvinov, V.I., Ivanova, A.S., and Devyatova, E.V., Generation of Arctic and Antarctic oscillations by torsional vibrations, *Solnechno-Zemnaya Fiz.*, 2009, no. 13, pp. 55–65.
- Mordvinov, V.I., Devyatova, E.V., Kochetkova, O.S., and Pogoreltsev, A.I., Simulation of stratospheric low-frequency disturbances, *RSHU Proceedings Journal*, 2011, no. 21, pp. 47–52.
- Mordvinov, V.I., Devyatova, E.V., Kochetkova, O.S., and Oznobikhina, O.A., Investigation of conditions for the generation and propagation of low-frequency disturbances in the troposphere, *Izv., Atmos. Ocean. Phys.*, 2013, vol. 49, no. 1, pp. 55–65.
- Palmeiro, F.M., Barriopedro, D., Herrera, R., and Calvo, N., Comparing sudden stratospheric warming definitions in reanalysis data, *J. Clim.*, 2015, vol. 28, pp. 6823–6840. doi 10.1175/JCLI-D15-0004.1
- Palmén, E. and Newton, C., *Atmospheric Circulation Systems*, New York: Academic, 1969; Leningrad: Gidrometeoizdat, 1973.
- Plumb, R.A., On the three-dimensional propagation of stationary waves, *J. Atmos. Sci.*, 1985, vol. 42, no. 3, pp. 217–229.
- Pogoreltsev, A.I., Generation of normal atmospheric modes by stratospheric vacillations, *Izv., Atmos. Ocean. Phys.*, 2007, vol. 43, no. 4, pp. 423–435.
- Pogoreltsev, A.I., Vlasov, A.A., Fröhlich, K., and Jacobi, Ch., Planetary waves in coupling the lower and upper atmosphere, *J. Atmos. Sol.-Terr. Phys.*, 2007, vol. 69, pp. 2083–2101. doi 10.1016/j.jastp.2007.05.014
- Pogoreltsev, A.I., Savenkova, E.N., and Pertsev, N.N., Sudden Stratospheric warmings: The role of normal atmospheric modes, *Geomagn. Aeron. (Engl. Transl.)*, 2014, vol. 54, no. 3, pp. 357–372.
- Pogoreltsev, A.I., Savenkova, E.N., Aniskina, O.G., Ermakova, T.S., Chen, W., and Wei, K., Interannual and intraseasonal variability of stratospheric dynamics and stratosphere–troposphere coupling during northern winter, *J. Atmos. Sol.-Terr. Phys.*, 2015, vol. 136, pp. 187–200.
- Ray, P. and Zhang, C., A case study of the mechanics of extratropical influence on the initiation of the Madden–Julian Oscillation, *J. Atmos. Sci.*, 2010, vol. 67, pp. 515–528.
- Rienecker, M.M., Suarez, M.J., Gelaro, R., et al., MERRA: NASA’s modern-era retrospective analysis for research and applications, *J. Clim.*, 2011, vol. 14, pp. 3624–3648. doi 10.1175/JCLI-D-11-00015.1
- Sheshadri, A., Plumb, R.A., and Gerber, E., Seasonal variability of the polar stratospheric vortex in an idealized AGCM with varying tropospheric wave forcing, *J. Atmos. Sci.*, 2015, vol. 72, pp. 2248–2266. doi 10.1175/JAS-D-14-0191.1
- Smith, A.K., Observation of wave–wave interaction in the stratosphere, *J. Atmos. Sci.*, 1983, vol. 40, pp. 2484–2496.
- Suvorova, E.N., Drobashevskaya, E.A., and Pogoreltsev, A.I., Clime model of three-dimensional ozone distributions according to MERRA reanalysis data, *Uch. Zap. Ross. Gos. Gidrometeorol. Univ.*, 2017, no. 49, pp. 38–46.
- Taguchi, M. and Hartmann, D.L., Increased occurrence of stratospheric sudden warmings during El Niño simulated by WACCM, *J. Clim.*, 2006, vol. 19, pp. 324–332. doi 10.1175/JCLI3655.1
- Vargin, P.A. and Volodin, E.M., Analysis of the reproduction of dynamic processes in the stratosphere using the climate model of the Institute of Numerical Mathematics, Russian Academy of Sciences, *Izv., Atmos. Ocean. Phys.*, 2016, vol. 52, no. 1, pp. 1–15.
- Weickmann, K.M., Lussy, G.R., and Kutzbach, J.E., Intraseasonal (30–60 day) fluctuations of outgoing longwave radiation and 250 mb stream function during northern winter, *Mon. Weather Rev.*, 1985, vol. 113, pp. 941–961.
- Welch, D.I., The generalization of “Student’s” problem when several different population variances are involved, *Biometrika*, 1947, vol. 34, no. 1, pp. 28–35.
- Wheeler, M.C. and Hendon, H.H., An all-season real-time multivariate MJO index: Development of an index for monitoring and prediction, *Mon. Weather Rev.*, 2004, vol. 132, pp. 1917–1932.

Translated by O. Ponomareva